SLAC-PUB-7173
hep-ph/9605462
May 1996

SIGNATURES OF COLOR-OCTET QUARKONIUM PRODUCTION[a]

M. BENEKE
Stanford Linear Accelerator Center, Stanford University,
Stanford CA 94309, U.S.A

I briefly review the nonrelativistic QCD picture of quarkonium production and its confrontation with experiment in various production processes.

1 Introduction

Quarkonium spectroscopy, decay and production has provided us with an interesting place to test our ideas on QCD ever since charmonium was discovered in 1974. Yet, the potential of perturbative QCD (PQCD) to treat production and decay has been fully exploited only recently [1] in a development comparable to that of Heavy Quark Effective Theory for heavy-light mesons. About the same time, experiments measuring quarkonium production at large transverse momentum have confronted theorists with surprizingly large cross sections. These observations have led to the understanding that fragmentation [2] and hadronization of color-octet [3,4] quark-antiquark ($Q\bar{Q}$) pairs are essential in the production process. Color-octet mechanisms were considered in quarkonium decays already a while ago [5]. They were found to solve the problem of infrared divergences in P-wave decays in a systematic way [6]. Taking them into account also in S-wave production, where they are not required by perturbative consistency in leading order of a nonrelativistic expansion, opens the promise of a quantitative description of quarkonium production.

In this talk I briefly summarize the concepts underlying the theory of quarkonium production. The subsequent survey of the importance of color-octet production concentrates on J/ψ production. [Of course, most results on direct J/ψ production generalize to $\psi(nS)$ and $\Upsilon(nS)$ states.] Because of space limitations, the presentation is sometimes sketchy and for many details

[a] To appear in the Proceedings of the Second Workshop on Continuous Advances in QCD, Minneapolis, U.S.A., March 1996. Research supported by the Department of Energy under contract DE-AC03-76SF00515.

the reader should consult the original literature, especially to appreciate the sources of uncertainty in comparing theory with experiment.

2 Theory of Quarkonium Production

2.1 Factorization

Inclusive quarkonium production involves two distinct scales. First, a heavy quark pair is produced on a distance scale of order $1/m_Q$. Then, the quark pair is bound into a quarkonium on a time scale of order of the inverse binding energy, $\tau \sim 1/(m_Q v^2)$ (in the quarkonium rest frame), where v is the typical velocity of the bound quarks. We assume that v^2 is small (but do not assume that the binding force is Coulombic). The creation process can be computed in PQCD and is insensitive to the details of the bound state. The binding process can not be computed perturbatively, but long-wavelength gluons responsible for binding do not resolve the short-distance production process. The factorization hypothesis for quarkonium production [1] states that the quarkonium production cross section can be written as a sum of short-distance coefficients that describe the creation of a $Q\bar{Q}$ pair in a state n multiplied by a process-independent matrix element that parameterizes the 'hadronization' of the $Q\bar{Q}$ state n into a quarkonium ψ plus light hadrons with energies of order $m_Q v^2$ in the quarkonium rest frame. Consequently, in a hadron-hadron collision $A + B \to \psi + X$, the differential cross section is given by

$$d\sigma = \sum_{i,j} \int dx_1 dx_2 \, f_{i/A}(x_1) f_{j/B}(x_2) \sum_n d\hat{\sigma}_{i+j \to Q\bar{Q}[n]} \, \langle \mathcal{O}_n^\psi \rangle, \qquad (1)$$

where $f_{i/A}$ denotes the parton distribution function. The factorization formula is diagrammatically represented in Fig. 1 for deeply inelastic scattering. The upper part of the diagram represents the matrix element $\langle \mathcal{O}_{\backslash}^\psi \rangle$. The hard part H is connected to this matrix element by $Q\bar{Q}$ lines plus additional lines, if $\mathcal{O}_n^\psi$ contains more fields. Factorization entails that soft gluons connecting S, H and the remnant jet J cancel up to 'higher twist' effects in Λ, where Λ represents the QCD low-energy scale. Each element in Eq. 1 depends on a factorization scale. Since gluon emission changes the $Q\bar{Q}$ state n, a change of factorization scale reshuffles contributions between different terms in the sum over n and only the sum is physical. The short-distance cross sections $d\hat{\sigma}$ are computed by familiar matching: One first calculates the cross section for a perturbative $Q\bar{Q}$ state and then subtracts the matrix elements computed in this state.

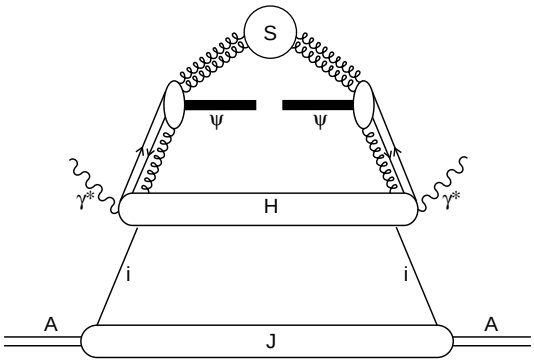

Figure 1: Diagrammatic representation of factorization in $\gamma^* + A \to \psi + X$. For the cross section the diagram has to be cut.

A heuristic argument for factorization can be given starting from the infrared finiteness of open heavy quark production. The above short-distance cross sections are obtained by expanding the amplitude squared for open heavy quark production in the relative three-momentum of the quarks and by taking projections on color and angular momentum states. Since soft gluon emission takes one from one state to another, each projection separately is not infrared safe. However, by construction the sum in n runs over all states, so that infrared sensitive contributions can always be absorbed in some matrix element. In this sense, the sum over all intermediate $Q\bar{Q}$ states restores the inclusiveness of open heavy quark production. It is also worth noting that Eq. 1 is valid, up to higher twist effects, even if the quarkonium is produced predominantly at small transverse momentum with respect to the beam axis, provided one integrates over all p_t. The transverse momentum distribution is not described by Eq. 1 unless $p_t \gg \Lambda$. A point of concern, however, is, that higher twist effects might be of order $\Lambda/(m_Q v^2)$, when a soft gluon from a remnant jet builds the higher Fock state $Q\bar{Q}g$ together with the quark pair. If these terms do not cancel, Eq. 1 would be quantitative in hadro-production of quarkonia at low p_t only for asymptotically large quark masses, since $\Lambda/(m_Q v^2) \sim 1$ both for charmonium and bottomonium.

2.2 NRQCD and Velocity Scaling

The matrix elements $\langle \mathcal{O}_n^\psi \rangle$ contain all interactions of the nonrelativistic $Q\bar{Q}$ pair (in its rest frame) with degrees of freedom with low momentum compared to m_Q. These interactions are accurately described by an effective field the-

ory called nonrelativistic QCD (NRQCD). The matrix elements are defined in NRQCD as [1]

$$\langle \mathcal{O}_n^H \rangle = \sum_X \sum_\lambda \langle 0| \chi^\dagger \kappa_n \psi |H(\lambda)X\rangle \langle H(\lambda)X| \psi^\dagger \kappa_n' \chi |0\rangle, \tag{2}$$

where the sum is over all polarizations λ and light hadrons X, and ψ, χ are two-spinor fields. [Matrix elements with additional gluon fields are suppressed in v^2 and will not be considered.] Typically, the 'kernels' κ_n, κ_n' specify the color, spin and orbital angular momentum state of the quark-antiquark pair.

Without an additional organizing principle, there would be too many matrix elements to make the theory predictive. The NRQCD Lagrangian informs us about the coupling of soft gluons to the $Q\bar{Q}$ pair. In particular, spin symmetry holds to leading order in v^2 and reduces the number of independent matrix elements considerably. There is no flavor symmetry as in Heavy Quark Effective Theory, because the kinetic energy term is part of the leading order Lagrangian. Quarkonium spectroscopy tells us that the kinetic energy is approximately constant in the range of reduced masses that comprises $c\bar{c}$ and $b\bar{b}$ states. Thus, $v^2 \sim 1/m_Q$ in the range of interest, while for very large quark masses $v^2 \sim 1/\ln^2 m_Q$. Furthermore, the overlap of the final state HX with a $Q\bar{Q}$ state n can be estimated from a multipole expansion, which allows us to drop some operators that acquire an additional suppression compared to the scaling in v^2 of the kernels themselves. The resulting 'velocity scaling rules' are summarized in Refs. [1,7]. The double expansion of a quarkonium production cross section in α_s and v^2 (neglecting higher twist corrections) is now complete.

As a result two matrix elements, $\langle \mathcal{O}_1^{\chi_{c0}}(^3P_0)\rangle$ and $\langle \mathcal{O}_8^{\chi_{c0}}(^3S_1)\rangle$ are needed to describe the production of all three P-wave states at leading order in v^2. The notation refers to the kernels in Eq. 2: The subscript denotes the color state and the angular momentum state is written in spectroscopic notation. The first matrix element reduces, to leading order in v^2, to the familiar derivative of the wavefunction at the origin. The second color-octet term absorbs the IR senstive regions that would otherwise appear in the short-distance cross section [3,6]. At leading order in v^2, J/ψ production is described by the single parameter $\langle \mathcal{O}_1^{J/\psi}(^3S_1)\rangle$. Because of charge conjugation, the gluon-gluon fusion short-distance cross section which multiplies this matrix element is suppressed by α_s and is proportional to α_s^3. Since $v^2 \sim 0.25 - 0.3$ is not very small for charmonium, higher order corrections in v^2 can be important, if they arise at lower order in α_s. According to the velocity scaling rules three color-octet matrix elements – $\langle \mathcal{O}_8^{J/\psi}(^3S_1)\rangle$, $\langle \mathcal{O}_8^{J/\psi}(^1S_0)\rangle$, $\langle \mathcal{O}_8^{J/\psi}(^3P_0)\rangle$ – contribute at order $\alpha_s^2 v^4$ (powers of v^2 are counted relative to the leading order contribution), so that J/ψ production is described by four nonperturbative parameters. Con-

tributions of order $\alpha_s^3 v^2$ also exist and can be important in specific regions of phase space. Because χ_{c1} production at low tranverse momentum is also suppressed by α_s compared to χ_{c0} and χ_{c2}, higher order corrections in v^2 would also be important for χ_{c1} production.

2.3 Fragmentation

We now consider the transverse momentum distribution $d\sigma/dp_t^2$. The leading order contributions (in α_s and v^2) decrease as $1/p_t^6$ (P-waves) or $1/p_t^8$ (S-waves), when p_t is large compared to $2m_Q$. This steep decrease is a penalty for preforming the quarkonium state at very small distances $1/p_t$ rather than $1/m_Q$ and is not what would be expected from a high-energy cross section in QCD. For $A + B \to H + X$, where H can be any hadron, we expect scaling: When the cms energy and p_t are large compared to all hadron masses, the short-distance cross section $d\hat{\sigma}/dp_t^2$ scales as $1/p_t^4$ on dimensional grounds, modulo logarithms of p_t and higher twist corrections of order m_H/p_t and Λ/p_t. Moreover, the leading twist cross section can be written as a convolution of distribution functions, a short-distance cross section and a fragmentation function. From their p_t-behaviour we deduce that the leading order (in α_s and v^2) J/ψ production mechanisms are higher twist at large p_t (but calculable, since m_H is large compared to Λ). In general, fragmentation functions remain uncalculable. If H is a quarkonium, however, the dependence on the energy fraction z can be calculated[2,8], because the quark mass $m_Q \gg \Lambda$ provides another large mass scale. Thus, a parton fragments first into a $Q\bar{Q}$ pair, which subsequently hadronizes. Since the hadronization of the $Q\bar{Q}$ pair takes place by emission of gluons with momenta of order $m_Q v^2$ in the quarkonium rest frame, the energy fraction of the quarkonium relative to the fragmenting parton, differs from that of the $Q\bar{Q}$ pair only by an amount $\delta z \sim v^2 \ll 1$. As a result, the fragmentation functions are expressed as a sum over perturbatively calculable, z-dependent coefficient functions that describe the fragmentation process $i \to Q\bar{Q}[n]$ multiplied by the same z-independent 'hadronization matrix elements' encountered earlier.

At large p_t quarkonium production depends on three small parameters: $\alpha_s/\pi \sim 0.1$, $v^2 \sim 0.25 - 0.3$, $4m_Q^2/p_t^2$ (numbers for charmonium). The leading contributions for octet vs. singlet and fragmentation vs. non-fragmentation production of J/ψ are shown in Tab. 1. The scaling with v^2 and $4m_c^2/p_t^2$ is measured relative to the color-singlet non-fragmentation term. We see that at $p_t \sim 10\,\mathrm{GeV}$ gluon fragmentation into a color-octet quark pair dominates[4] all other mechanisms by at least a factor ten.

Table 1: Parametric dependence of various J/ψ production mechanisms in hadron-hadron collisions.

	color singlet	color octet
$p_t \sim 0$	α_s^3	$\alpha_s^2 v^4$
$p_t \gg 2m_Q$	$\alpha_s^5 \left(p_t^2/(4m_Q^2)\right)^2$	$\alpha_s^3 v^4 \left(p_t^2/(4m_Q^2)\right)^2$

2.4 Quarkonium Polarization

Quarkonium polarization in the NRQCD formalism has been considered in Refs. [9,10,11,12]. A novel feature as compared to unobserved polarization is that the short-distance cross sections can not be determined from a matching calculation that involves only amplitudes squared of $Q\bar{Q}$ states with definite angular momentum. The final quarkonium state can be reached through quark-antiquark pairs in various spin and orbital angular momentum states, which are coherently produced, so that interference between different intermediate states occurs [9,11,12]. Because of parity and charge conjugation symmetry, intermediate states with different spin S and angular momentum L can not interfere, so that for J/ψ production interference occurs for intermediate ${}^3P_J$-states only. The interference terms are crucial to obtain a factorized expression for fragmentation functions into polarized $\psi(nS)$ states [9].

The amplitude projections that determine the short-distance cross section can be found as follows. The cross section can be written as (see Fig. 1)

$$\sigma^{(\lambda)} \sim H_{ai;bj} \cdot S^{(\lambda)}_{ai;bj} \,, \tag{3}$$

where the indices ij and ab refer to spin and orbital angular momentum in a Cartesian basis $L_a S_i$ $(a, i = 1, 2, 3 = x, y, z)$. For $Q\bar{Q}$ with spin and orbital angular momentum one, the soft part is given by

$$S^{(\lambda)}_{ai;bj} = \sum_X \langle 0|\chi^\dagger \sigma_i T^A \left(-\frac{i}{2}\overleftrightarrow{D}_a\right)\psi \,|J/\psi(\lambda)X\rangle\langle J/\psi(\lambda)X|\, \psi^\dagger \sigma_j T^A \left(-\frac{i}{2}\overleftrightarrow{D}_b\right)\chi|0\rangle \,, \tag{4}$$

where helicity λ is fixed. To proceed one writes down the most general tensor decomposition compatible with rotational invariance, parity and charge conjugation. In general, this introduces a substantial number of new nonperturbative parameters. To evaluate the matrix element at leading order in v^2, we may use spin symmetry. Spin symmetry implies that the spin of the J/ψ

is aligned with the spin of the $c\bar{c}$ pair, so $S^{(\lambda)}_{ai;bj} \propto \epsilon^{i*}(\lambda)\epsilon^{j}(\lambda)$. One then finds

$$S^{(\lambda)}_{ai;bj} = \langle \mathcal{O}_8^{J/\psi}(^3P_0)\rangle \, \delta_{ab} \, \epsilon^{i*}(\lambda)\epsilon^{j}(\lambda)\,. \tag{5}$$

All other possible Lorentz structures are suppressed by v^2. Moreover, the single surviving structure is related to a matrix element that appeared already in unpolarized production. This result is general[9,11,12]: At order $\alpha_s^2 v^4$, no new matrix elements are required to describe J/ψ polarization.

The decomposition Eq. 5 tells us that to calculate the polarized production rate we should project the hard scattering amplitude onto states with definite $S_z = \lambda$ and L_z, square the amplitude, and then sum over L_z ($\sum_{L_z} \epsilon_a(L_z)\epsilon_b(L_z) = \delta_{ab}$ in the rest frame). The soft part is diagonal in the $L_z S_z$ basis. It is straightforward to transform to the more conventional JJ_z basis. Since $J_z = L_z + S_z$, there is no interference between intermediate states with different J_z. We write, with obvious notation,

$$\sigma^{(\lambda)} \sim \sum_{JJ_z;J'J'_z} H_{JJ_z;J'J'_z} \cdot S^{(\lambda)}_{JJ_z;J'J'_z}\,, \tag{6}$$

and obtain, using Eq. 5,

$$S^{(\lambda)}_{JJ_z;J'J'_z} = \langle \mathcal{O}_8^{J/\psi}(^3P_0)\rangle \sum_M \langle 1M;1\lambda|JJ_z\rangle\langle J'J'_z|1M;1\lambda\rangle\,, \tag{7}$$

which is diagonal in $(JJ_z)(J'J'_z)$ only after summation over λ (unpolarized production). In general, the off-diagonal matrix elements cause interference of the following JJ_z states: 00 with 20, 11 with 21 and $1(-1)$ with $2(-1)$. This particular pattern of interference is a consequence of spin symmetry. In general, all states interfere, and diagonality in the $L_z S_z$ basis is also lost.

3 Confrontation with Experiment

The interest in color-octet production mechanisms was ignited by the possibility to explain the large ψ' production cross section at the Tevatron by gluon fragmentation into a color-octet $c\bar{c}$ pair. Over the past year most J/ψ production processes have been reanalyzed with color-octet mechanisms taken into account. In this section I intend to give a short summary. References to experimental results can be found in the quoted papers. The letter 'ψ' denotes J/ψ and ψ' collectively.

3.1 Large p_t

Quarkonium production at large transverse momentum with respect to the beam axis can be measured at colliders, most recently in $p\bar{p}$ collisions at the Tevatron, where the indirect contribution from B decays can be removed. The accessible range of p_t is $5\,\mathrm{GeV} < p_t < 20\,\mathrm{GeV}$. In this range fragmentation dominates. The J/ψ production data, which includes feed-down from P-wave states could be described [13] - within theoretical and experimental errors - by fragmentation into P-wave states together with color-singlet gluon fragmentation into J/ψ. The ψ' cross section, however, is under-predicted by a factor 30 by color singlet fragmentation. The same deficit was found for direct J/ψ production, after the contributions from higher charmonium states could be separated. The dominant S-wave production mechanism was still missed.

The discrepancy can be explained [4,14] by taking into account that a gluon can fragment into a color octet $c\bar{c}$ pair in a ${}^3S_1$ state, which decays into a ψ state by emission of two gluons with momenta of order $m_c v^2$ in the quarkonium rest frame. The suppression factor v^4 is more than compensated by the enhanced short-distance coefficient, see Tab. 1 and Sect. 2.3. At lowest order in α_s only $\langle \mathcal{O}_8^\psi({}^3S_1)\rangle$ is probed by gluon fragmentation and can be determined by fitting the Tevatron data. The resulting $\langle \mathcal{O}_8^\psi({}^3S_1)\rangle / \langle \mathcal{O}_1^\psi({}^3S_1)\rangle \sim 1/100$ is actually smaller than $v^4 \sim 1/10$ as expected from velocity scaling. Apart from numerical factors in the short-distance coefficients, this could partly be due to the fact that the emission of soft gluons is kinematically not accounted for in the octet fragmentation function. Soft gluon emission softens the fragmentation function by smearing the delta-function over a region $\delta z \sim v^2$ in longitudinal momentum fraction. Since the short-distance cross section falls off like $1/p_t^4$, one roughly probes the fourth moment of the fragmentation function. A softer fragmentation function would then require a larger matrix element to fit the data.

The theoretical predicition was extended to moderate $p_t \sim 2m_c$ (or slightly larger) in Ref. [15], where contributions suppressed by $4m_c^2/p_t^2$ at large p_t have been kept. In this intermediate region, all three color-octet matrix elements relevant for ψ production are equally significant, but should be suppressed by v^4 compared to the color-singlet cross section, since no compensating factors of π/α_s are at work. Surprizingly, due to numerical enhancements of the amplitudes, the color-octet contributions still dominate and seem to be required to describe the data. The best fit yields a value of $\langle \mathcal{O}_8^{J/\psi}({}^3S_1)\rangle$ which is more than a factor two smaller than the one extracted [14] from large p_t, while the fitted combination of $\langle \mathcal{O}_8^{J/\psi}({}^3P_0)\rangle$ and $\langle \mathcal{O}_8^{J/\psi}({}^1S_0)\rangle$ is rather large, especially in comparison with the fits for ψ'. Whether this difference between J/ψ and

ψ' is an artefact or physical effect remains to be decided.

As noted in Ref. [16], the above scenario implies, that the directly produced ψ mesons are almost completely transversely polarized at large p_t. The fragmenting gluon is transversely polarized and transfers its polarization to the $c\bar{c}$ pair in the ${}^3S_1$ state. Because of spin symmetry, the transverse polarization stays intact in the emission of two soft gluons. Polarization would be measured in the angular distribution of leptonic ψ decay, $d\Gamma/d\cos\theta \propto 1+\alpha\cos^2\theta$, where θ denotes the angle between the lepton three-momentum in the ψ rest frame and the ψ three-momentum in the lab frame. Higher order corrections to the fragmentation function can result in longitudinally polarized ψ, but were found to be rather small [9]. For $\langle\mathcal{O}_8^\psi({}^3P_0)\rangle/(m_c^2\langle\mathcal{O}_8^\psi({}^3S_1)\rangle) < 2$, one still has $\alpha > 0.64$. Spin-symmetry breaking corrections are suppressed by v^4 and introduce an uncertainty of 0.1 in α. These corrections to $\alpha = 1$ persist at large p_t. For moderate p_t corrections that vanish as $4m_c^2/p_t^2$ exist, but have not yet been calculated. Since other corrections are small, these could well dominate over most of the p_t-range accessible at the Tevatron. So far, the angular distribution remains unmeasured. There is a price in statistics to pay, but understanding the angular dependence of the detector acceptance is also non-trivial. Ideally, a measurement of the p_t-dependence of α will provide a decisive self-consistency test of the octet production picture.

At HERA large-p_t production of J/ψ is probed in γp collisions. In this case gluon fragmentation plays no role, since at leading order in α_s only γq collisions contribute to this mechanism. Color singlet charm fragmentation, induced by photon-gluon fusion, dominates [17] at large p_t.

3.2 Small p_t: Fixed Target Experiments

Fixed target experiments have for a long time been the most profuse source of quarkonium production data. Since no cut on p_t is usually imposed, the production cross section is dominated by quarkonia with transverse momenta of about 1 GeV. The cms energies range up to $\sqrt{s} = 40$ GeV. The most recent comparisons of color-singlet production mechanisms with data are documented in Refs. [18,19]. Summarizing the conclusions of Ref. [19], the color singlet mechanisms (a) do not account for the over-all normalization of the total cross section very well, (b) yield too low a fraction of directly produced J/ψ, (c) transverse rather than no polarization of J/ψ and ψ and (d) predict far too few χ_{c1} states in comparison to χ_{c2}. With these failures in mind, color-octet mechanisms have been analyzed [11,20,21]. [For reasons explained in Ref. [11], there are substantial differences in numerics and conclusions between these three analyses. The subsequent presentation adheres to Ref. [11].] The results are not

entirely encouraging, but not uninteresting either.

Because of charge conjugation, color-singlet ψ production is suppressed by α_s. Consequently, octet mechanisms scale as $(\pi/\alpha_s)\, v^4 \sim 1$, see Tab. 1. Since the color-singlet amplitude vanishes at $c\bar{c}$ threshold while the octet amplitude does not, and since the cross section is enhanced at threshold by the x-behaviour of the gluon distribution, color-octet production actually dominates the cross section. At leading order, the combination $\Delta_8(\psi) = \langle \mathcal{O}_8^\psi(^1S_0)\rangle + 7/m_c^2 \langle \mathcal{O}_8^\psi(^3P_0)\rangle$ is probed. At this order $\langle \mathcal{O}_8^\psi(^3S_1)\rangle$ arises only in $q\bar{q}$ annihilation, which is numerically small compared to gluon-gluon fusion in the energy range considered.

Starting with total unpolarized cross sections, one has three observables - $\sigma_{J/\psi}$, $\sigma_{\psi'}$ and the direct J/ψ cross section $\sigma_{J/\psi}^{dir}$, which does not include feed-down from higher charmonium states - and two octet hadronization parameters - $\Delta_8(J/\psi)$, $\Delta_8(\psi')$ - to fit. [If these were accurately known from other processes, no free parameter would remain.] Such a fit is possible with matrix elements consistent with their expected size from velocity scaling. The energy dependence of the total cross section is in agreement with the data, although this can not be considered very significant. A fit to $\sigma_{J/\psi}$ and $\sigma_{\psi'}$ then predicts a direct J/ψ production fraction of about 60%, in good agreement with experiment. With respect to the failures (a) and (b) above, this could be considered as strong evidence for important color-octet contributions in direct ψ production. The uncertainties, however, are appreciable. For example, in the above fit, the color-singlet matrix elements were taken from Buchmüller-Tye wavefunctions at the origin and not considered as free parameters. The overall normalization depends strongly on the charm quark mass, although the direct production fraction does not. The short-distance coefficients have been expressed in terms of the charm quark mass rather than quarkonium masses. This is conceptually preferred by the factorization formalism and numerically quite important.

Even disregarding these uncertainties, the above picture can not be considered as complete. Defining a parameter α for the angular distribution as before, where θ is now the angle between the three-momentum vector of the positively charged muon and the beam axis in the quarkonium rest frame, one finds $0.15 < \alpha < 0.44$ for ψ' production at $\sqrt{s} = 21.8\,\mathrm{GeV}$ and $0.31 < \alpha < 0.63$ for J/ψ production at $\sqrt{s} = 15.3\,\mathrm{GeV}$. [Since the energy dependence is mild, these numbers can be used with little error at higher cms energies.] These estimates could be made more precise, if the matrix elements $\langle \mathcal{O}_8^{J/\psi}(^3P_0)\rangle$ and $\langle \mathcal{O}_8^{J/\psi}(^1S_0)\rangle$ were individually known. The degree of transverse polarization is higher in J/ψ production, because the indirect contribution from χ_{c2} decays yields a purely transversely polarized component to the cross section. These

estimates should be compared with the measurement of no visible polarization, $\alpha \approx 0$, both for ψ' and J/ψ.

At leading order in v^2, one predicts a $\chi_{c1} : \chi_{c2}$ production ratio (weighted by their branching fractions to decay into J/ψ) of $1 : 7$, mainly because χ_{c1} production is suppressed in α_s. As for direct J/ψ production, higher order corrections in v^2 can be expected to dominate χ_{c1} production. Although they have not yet been analyzed, they could raise the above ratio to about $1 : 3$, still far below the observed ratio $(1.4 \pm 0.4) : 1$. Since the $\chi_{c1} : \chi_{c2}$ ratio has been measured in only one experiment [22], an independent confirmation of this discrepancy would be welcome.

The discrepancy between predictions and data on polarization might be due to numerically large spin symmetry breaking corrections, which would lead to less transverse polarization. One could also suspect that the experiments have not yet fully accounted for all systematic errors. In the E672/E706 experiment (the only one that provides this piece of information [23]), for instance, the acceptance and efficiency varies strongly with angle, while at the same time, the acceptance/efficiency curve was determined from a Monte Carlo sample of unpolarized quarkonia. However, together with the problematic $\chi_{c1} : \chi_{c2}$ ratio, it seems more likely that the interactions of a color octet $c\bar{c}$ pair with soft gluons as it traverses the target are not understood. Although of higher twist in Λ/m_c, such effects must be sizeable as illustrated by the large nuclear dependence of the total ψ cross sections, which is dynamically also not understood. Since quarkonium formation occurs only after the $c\bar{c}$ pair left the nucleus, it appears as if by the time the quarkonium is formed, the $c\bar{c}$ pair has lost 'memory' that it was produced from two on-shell (transverse) gluons, as assumed in leading twist. But even if higher twist effects are sizeable, the polarization problem seems hard to solve, since the coupling of soft gluons to the $c\bar{c}$ pair would be subject to spin symmetry and the counting rules for multipole transitions, so that transverse polarization is again hard to avoid. No higher twist mechanism has yet been shown to produce predominantly longitudinal polarization in the central x_F region that dominates the cross section. To clarify the higher twist nature of the discrepancies, analogous measurements for Υ production would be desirable. As another check, it would be interesting to know to what extent χ_{c2} is produced with helicity ± 2 as predicted at leading twist (with small corrections).

Photoproduction of charmonia in fixed target experiments (or HERA, in the low-p_t region) is theoretically rather similar to fixed target hadroproduction as far as the underlying diagrams and the probed matrix element $\Delta_8(J/\psi)$ is concerned. A comparison of octet mechanisms with data was undertaken both in the elastic region [24,25,26] $z > 0.95$ and the inelastic domain [24,26] $z < 0.9$,

where $z = p\cdot k_\psi / p\cdot k_\gamma$ is the energy fraction E_ψ/E_γ in the proton rest frame. In the elastic region color-octet contributions are enhanced by π/α_s compared to color-singlet contributions, as in fixed target hadroproduction. The extracted matrix element $\Delta_8(J/\psi)$ is consistent with the extraction from hadroproduction, but substantially smaller than what would have been expected from the fit to the Tevatron data in the moderate p_t domain discussed earlier. While the consistency with hadroproduction is reassuring, the situation with higher twist effects is even more delicate in the large-z region than in hadroproduction. As octet mechansims, 'diffractive' quarkonium production is also centered at $z \approx 1$ and unsuppressed if not dominant in the endpoint region. In addition, the restriction $z > 0.95$ might not allow the process to be sufficiently inclusive, as is necessary in the NRQCD approach. With these remarks of caution in mind, the discrepancy in color-octet matrix elements between 'high' energy (Tevatron) and 'low' energy fits should probably not be over-interpreted. It is likely that energy dependent higher-order radiative corrections (such as small-x effects) would, once taken into account, lower the matrix elements extracted from the Tevatron fits. Such a reduction would be welcome to explain a factor two discrepancy in comparison with large-p_t UA1 data [14] and the J/ψ branching fraction in B decays, see below.

In the inelastic domain $z < 0.9$, color-octet processes are parametrically suppressed by v^4, but, due to enhancements in the amplitudes, numerically of the same order as color-singlet processes. When z approaches unity, the color-octet contributions diverge as expected from a partonic process with a lowest order term proportional to $\delta(1-z)$. This divergence indicates that the partonic prediction must be considered as a distribution. When smearing is applied, together with the constraints on the matrix elements $\langle \mathcal{O}_8^{J/\psi}(^3P_0)\rangle$ and $\langle \mathcal{O}_8^{J/\psi}(^1S_0)\rangle$ from the elastic peak, the presence of color-octet contributions does not appear to be in conflict with the J/ψ energy distribution in fixed target experiments or at HERA.

3.3 e^+e^- Annihilation and Z^0 Decay

Quarkonium production in e^+e^- annihilation shows much of the variety of production mechanisms in hadro- and photoproduction, while eliminating the uncertainties related to hadrons in the initial state. On the other hand, the cross sections are not large and there is not much data to compare with. [For instance, out of 3.6 million hadronic Z^0 decays, OPAL has found 24 prompt J/ψ.]

The situation when $\sqrt{s}$ is not much larger than $2m_c$, relevant at CLEO, has been investigated in Ref. [27]. The parametric dependence of color-octet

contributions to the charmonium energy spectrum is analogous to the energy spectrum in photoproduction. At leading order in α_s, the $c\bar{c}$ pair can only be produced in an octet state, which should be seen as a jet containing a charmonium, recoiling against a gluon jet. The energy distribution is peaked at the endpoint $E_{max} = (s + M_\psi^2)/(2\sqrt{s})$, a delta-function smeared over a region $v^2 E_{max}$. Away from the endpoint, color-singlet contributions are more important. In addition to the energy spectrum, the J/ψ angular distribution leads to a striking signature of octet production: Close to the endpoint of the energy spectrum, color-singlet production favors J/ψ production perpendicular to the beam axis, while octet mechanisms produce J/ψ predominantly along the beam axis. An accurate prediction again requires the values of the matrix elements $\langle \mathcal{O}_8^{J/\psi}(^3P_0)\rangle$ and $\langle \mathcal{O}_8^{J/\psi}(^1S_0)\rangle$.

When $s \gg 4m_c^2$, as relevant for Z^0 decay at LEP, the production patterns change. The ratio $4m_c^2/M_Z^2$ is now an important parameter, just as $4m_c^2/p_t^2$ at large p_t. The dominant production mechanisms are of fragmentation-type. Although suppressed by v^4 compared to color-singlet charm fragmentation, gluon fragmentation into a color-octet $c\bar{c}$ pair in a $^3S_1$ state wins [28,29] over charm fragmentation by a factor of approximately three, depending on the choice of values for the color-singlet and octet matrix elements. Gluon fragmentation benefits from larger color and flavor factors (all $Z^0 \to q\bar{q}$ initiate gluon fragmentation), but most importantly from a double logarithmic enhancement in $4m_c^2/m_Z^2$ from the phase space region, where the fragmenting gluon is collinear to and softer than the primary quark. Consequently, color-octet gluon fragmentation could be discriminated from charm fragmentation that yields more energetic charmonia [28].

Present data from LEP [30] have too low statistics to idenitfy a gluon fragmentation contribution unambiguously. The central value for the prompt J/ψ branching fraction $\mathrm{Br}(Z^0 \to J/\psi\,\mathrm{prompt} + X) = (1.9 \pm 0.7 \pm 0.5 \pm 0.5) \cdot 10^{-4}$ however, is about a factor of two larger than the sum of all color-singlet contributions. [Such statements are not quite exact, since the experimental efficencies and thus results depend on the assumptions on the underlying production mechanism. The largest experimental error arises from the determination of the prompt production fraction.] The measured energy spectrum is neither peaked towards low energies nor towards large energies. Closing the eyes on the present errors, one would suspect a roughly equal contribution from charm and color-octet gluon fragmentation.

3.4 Bottom Decay

Color-octet mechanisms have been first considered for the inclusive χ_{cJ} yield in B meson decays [3]. In leading logarithmic approximation, color singlet production is proportional to $(2C_+ - C_-)^2 \approx 0.16$, while octet production is proportional to $(C_+ + C_-)^2 \approx 4.9$, where C_+ and C_- are related to the Wilson coefficients of the current-current operators in the $\Delta B = 1$ effective Hamiltonian. This numerical enhancement in the Wilson coefficients allows color-octet contributions to compete with color-singlet contributions, even though the first are suppressed by v^4 in the matrix elements[26,31]. The measured branching fraction $\mathrm{Br}(B \to J/\psi + X) = (0.80 \pm 0.08)\%$ allows us, in principle, to put a bound on the least known matrix elements $\langle \mathcal{O}_8^{J/\psi}(^3P_0)\rangle$ and $\langle \mathcal{O}_8^{J/\psi}(^1S_0)\rangle$. But the cancellations in the combination $(2C_+ - C_-)^2$ also render its numerical value highly sensitive to the choice of scale in the Wilson coefficients. This, together with the uncertainties in the wavefunction at the origin, leave an uncertainty of about a factor four in the color-singlet contribution. However, even with no color-singlet contribution at all and no contribution from $\langle \mathcal{O}_8^{J/\psi}(^3S_1)\rangle$, the Tevatron fit [15] of $\langle \mathcal{O}_8^{J/\psi}(^1S_0)\rangle + 3/m_c^2 \langle \mathcal{O}_8^{J/\psi}(^3P_0)\rangle \sim 6.5 \cdot 10^{-2}$ would overestimate the branching fraction by about 50%. Thus, B decays favor the smaller values of these matrix elements inferred from fixed target hadro- and photoproduction.

Bottomonium decay provides another J/ψ production process. The two most important production mechanisms are [32,33] $\Upsilon \to \chi_{cJ} + X$, dominated by octet χ_{cJ} production, followed by radiative χ_{cJ} decay, and $\Upsilon \to ggg^*$, followed by $g^* \to c\bar{c}[^3S_1^{(8)}]$. The second mechanism is similar to color-octet gluon fragmentation, although the Υ mass is not large enough to justify the fragmentation approximation. The branching fractions are estimated to be $7 \cdot 10^{-5}$ and $2.5 \cdot 10^{-4}$, respectively, using the larger value $\langle \mathcal{O}_8^{J/\psi}(^3S_1)\rangle = 0.015\,\mathrm{GeV}^3$. Their sum is only a factor of two below the upper bound $6.8 \cdot 10^{-4}$ from ARGUS and consistent with the CLEO result $(1.1 \pm 0.4) \cdot 10^{-3}$ within 2σ.

4 Conclusion

The magnitude of color-octet vs. color-singlet production cross sections for the J/ψ production processes discussed in Sect. 3 are summarized in brief in Tab. 2, together with the hadronization matrix elements probed in the corresponding process. A rather striking observation is that color-octet mechanisms dominate every production process. So, why are we discussing them only more than twenty years after the discovery of charmonium?

Table 2: Importance of color octet contributions in various J/ψ production processes and the octet matrix elements that could be probed in the corresponding process.

Process	Reference	$\frac{\text{octet}}{\text{singlet}}$	Matrix elements
$p\bar{p}$, large p_t	Ref. [4,14]	30	${}^3S_1^{(8)}$
$p\bar{p}$, moderate p_t	Ref. [15]	8	${}^3S_1^{(8)}$, ${}^3P_0^{(8)}$, ${}^1S_0^{(8)}$
Hadroproduction, fixed target	Ref. [11,20,21]	2-8	${}^3P_0^{(8)}$, ${}^1S_0^{(8)}$
Photoproduction, $z > 0.95$	Ref. [24,25,26]	4	${}^3P_0^{(8)}$, ${}^1S_0^{(8)}$
Photoproduction, $z < 0.9$	Ref. [24,26]	1	${}^3P_0^{(8)}$, ${}^1S_0^{(8)}$
Z^0 decay	Ref. [28,29]	3	${}^3S_1^{(8)}$
e^+e^- annihilation, large z	Ref. [27]	4	${}^3P_0^{(8)}$, ${}^1S_0^{(8)}$
B decay	Ref. [26,31]	3	${}^3S_1^{(8)}$, ${}^3P_0^{(8)}$, ${}^1S_0^{(8)}$
Υ decay	Ref. [32,33]	3	${}^3S_1^{(8)}$

For one thing, many accurate experimental results are rather recent. Another is that the charm mass is not really large enough to make precise predictions. Thus, a dramatic signature such as in large-p_t production at the Tevatron was necessary to induce a reanalysis of other processes. The numbers in the table should be considrered as indicative only and are often uncertain by a factor of two or more. Even now these uncertainties do not allow us to determine all production matrix elements. With the correct theoretical framework at hand, further effort, both experimental and theoretical, can be undertaken to make the presented quarkonium production picture fully quantitative.

Acknowledgements

I wish to thank Ira Rothstein for his collaboration on the subject discussed in this article and Arthur Hebecker for very useful discussions. Thanks to both for reading the manuscript.

References

1. G.T. Bodwin, E. Braaten and G.P. Lepage, *Phys. Rev.* D **51**, 1125 (1995)
2. E. Braaten and T.C. Yuan, *Phys. Rev. Lett.* **71**, 1673 (1993)
3. G.T. Bodwin, E. Braaten and G.P. Lepage, *Phys. Rev.* D **46**, 3703 (1992)
4. E. Braaten and S. Fleming, *Phys. Rev. Lett.* **74**, 3327 (1995)
5. M.B. Voloshin, *Sov. J. Nucl. Phys.* **40**, 662 (1984)
6. G.T. Bodwin, E. Braaten and G.P. Lepage, *Phys. Rev.* D **46**, 1914 (1992)
7. G. P. Lepage, L. Magnea, C. Nakleh, U. Magnea and K. Hornbostel, *Phys. Rev.* D **46**, 4052 (1992)
8. J.P. Ma, *Phys. Lett.* B **332**, 398 (1994)
9. M. Beneke and I.Z. Rothstein, *Phys. Lett.* B **372**, 157 (1996)
10. J.P. Ma, *Nucl. Phys.* B **460**, 109 (1996)
11. M. Beneke and I.Z. Rothstein, SLAC-96-7129, to appear in *Phys. Rev.* D [hep-ph/9603400]
12. E. Braaten and Y.-Q. Chen, OHSTPY-HEP-T-96-010 [hep-ph/9604237]
13. M. Cacciari and M. Greco, *Phys. Rev. Lett.* **73**, 1586 (1994); E. Braaten, M. Doncheski, S. Fleming and M. Mangano, *Phys. Lett.* B **333**, 548 (1994); D.P. Roy and K. Sridhar, *Phys. Lett.* B **339**, 141 (1994);
14. M. Cacciari, M. Greco, M.L. Mangano and A. Petrelli, Phys. Lett. **B356**, 553 (1995)
15. P. Cho and A.K. Leibovich, *Phys. Rev.* D **53**, 150 (1996); *Phys. Rev.* D **53**, 6203 (1996)
16. P. Cho and M.B. Wise, *Phys. Lett.* B **346**, 129 (1995)
17. R.M. Godbole, D.P. Roy and K. Sridhar, *Phys. Lett.* B **373**, 328 (1996)
18. G.A. Schuler, CERN-TH-7170-94 [hep-ph/9403387]
19. M. Vänttinen, P. Hoyer, S.J. Brodsky and W.-K. Tang, *Phys. Rev.* D **51**, 3332 (1995)
20. W.-K. Tang and M. Vänttinen, *Phys. Rev.* D **53**, 4851 (1996); NORDITA-96/18 P [hep-ph/9603266]
21. S. Gupta and K. Sridhar, TIFR/TH/96-04 [hep-ph/9601349]
22. Y. Lemoigne *et al.*, *Phys. Lett.* B **113**, 509 (1982)
23. A. Gribushin *et al.*, *Phys. Rev.* D **53**, 4723 (1996)
24. M. Cacciari and M. Krämer, DESY 96-005 [hep-ph/9601276]
25. J. Amundson, S. Fleming and I. Maksymyk, UTTG-10-95 [hep-ph/9601298]
26. P. Ko, J. Lee and H.S. Song, Seoul University report [hep-ph/9602223]
27. E. Braaten and Y.-Q. Chen, *Phys. Rev. Lett.* **76**, 730 (1996)
28. K. Cheung, W.-Y. Keung and T.C. Yuan, *Phys. Rev. Lett.* **76**, 877

(1996)
29. P. Cho, *Phys. Lett.* B **368**, 171 (1996)
30. The OPAL collaboration, CERN-PPE/96-062, to appear in *Phys. Lett.* B
31. P. Ko, J. Lee and H.S. Song, *Phys. Rev.* D **53**, 1409 (1996)
32. H.D. Trottier, *Phys. Lett.* B **320**, 145 (1994)
33. K. Cheung, W.-Y. Keung and T.C. Yuan, FERMILAB-PUB-96-027-T, to appear in *Phys. Rev.* D [hep-ph/9602423]